HT2019-3734

LIQUID TRANSPORT DURING EVAPORATION OF WATER FROM A SMALL SIMULATED SOIL COLUMN

Partha Pratim Chakraborty, Molly Ross, Hitesh Bindra, and Melanie M. Derby¹

Department of Mechanical and Nuclear Engineering Kansas State University Manhattan, KS

ABSTRACT

The food-energy-water nexus considers critical resource challenges which must be resolved in order to meet the needs of a growing population. Agriculture is the largest global water user, accounting for two-thirds of global water withdrawals, including water for crop irrigation. Understanding and therefore reducing evaporation of water from soil is an approach to conserve water resources globally. This work studies evaporation of water from a simulated soil column and employs x-ray imaging to determine the location of water in the porous media. A 30-mL beaker was filled with approximately 1700 2-mm hydrophilic glass beads. Water (i.e., 5.5 mL) was added to the simulated soil, comprised of glass beads and a heat flux (i.e., 1500 W/m²) was applied to the beaker using a solar simulator and the intensity was measured with a light meter. Real-time mass measurements were recorded during evaporation and X-ray imaging was utilized to capture liquid transport during evaporation. Images were post-processed using Matlab; the position of the liquid front was determined from this imaging. Across three replications, it took 47 hours on average to evaporate 5 mL of the total 5.5 mL of water. The transitions between evaporation Stage I, II, and III evaporation rates were determined using mass data and x-ray imaging; transition between Stages I and II occurred between approximately 4 and 9 hours, and the transition from Stage II to III evaporation occurred between approximately 18 and 24 hours. The result of this experiment will be useful to understand the liquid transport and formation of liquid bridges during evaporation from soil.

Keywords: Stage one evaporation, stage two evaporation, x-ray imaging, porous media, food-energy-water, INFEWS, transient

1. INTRODUCTION

Innovations in the food, energy, and water nexus are required to feed a growing population, projected to reach 9.8 billion population in 2050 [1], with fewer resources (e.g., no new arable land, less water and energy, etc.). Worldwide, agriculture is the largest water use and is responsible for two-thirds of water withdrawals [2].

Central High Plains, a semi-arid region in the midwestern United States which is an agricultural powerhouse [3, 4]. The region faces significant challenges as the Ogallala aquifer level declines; water levels have dropped 7 m over the last decade and natural recharge rates would take hundreds of years to refill the depleted aquifer [4-7]. This research seeks to understand evaporation mechanisms in order to design interventions to reduce soil evaporation rates and, therefore, required irrigation.

Three stages of evaporation are typically present in soils and

The Ogallala aquifer is the primary irrigation source for the

Three stages of evaporation are typically present in soils and evaporation from this three-phase (i.e., air, water, and soil) system depends on environmental conditions, soil type, pore size, and water content [8-13]. In Stage I evaporation, adequate water is available at the soil surface and the process is rate-limited by evaporation at the given environmental conditions (i.e., air temperature, relative humidity, and radiation), similar to evaporation from a pan of water [14, 15]. As the top layer of water in the soil evaporates, evaporation transitions from Stage I to Stage II evaporation. In field systems, Stage II evaporation begins in a time frame of hours to days. The soil experiences partial dryout in the upper level of the soil and evaporation rates decrease with respect to time. Stage II evaporation is typically limited by water transport to the surface through capillary action (i.e., replenishment of water to the upper soil surface) [16-22]. Often the largest decrease in time-based evaporation rate occurs while Stage II evaporation progresses. Finally, in Stage III evaporation, nearly total dry-out occurs in the top portion of the soil, and evaporation is driven by enhanced vapor diffusion. Vapor diffusion rates are often 1.5-5 times that predicted by Fick's diffusion law [9, 23-27] and are termed enhanced vapor diffusion.

The research objectives of this study are to investigate evaporation stages in a small, simulated soil column using X-ray imaging. X-ray imaging provides an excellent opportunity to determine the location of the drying front and, combined with real-time mass measurements, identify the location of water in the porous media, evaporation stages, and evaporation mechanisms.

¹ Contact author: derbym@ksu.edu

2. EXPERIMENTAL APPARATUS

Evaporation of deionized water was observed from a simulated soil column created with hydrophilic glass beads placed in a column. Experiments were conducted in a quiescent atmosphere where the relative humidity (RH) was 35% (maximum deviation of 2% RH) and the temperature was 22.2 °C (maximum deviation of 2°C) at atmospheric pressure. The relative humidity and temperature were measured every 30 minutes with a RH 62F rugged hygrometer with a resolution of 0.1%.

A total of 5.5 mL of water were added to a 2-cm-diameter, 3cm-tall beaker. The mass and volume of water was kept constant using a 2-13 mL volumetric dropper. A sensitive scale (FX-1200i) was used to measure the mass of the system and subsequent mass loss of the water due to evaporation. The scale has a capacity of 1200 grams with an uncertainty of \pm 0.01 grams. Initially, the beaker was placed on the scale to measure its mass (i.e., 8.03 grams). Then, the beaker was filled with 2-mmdiameter the mass was measured again (i.e., 24.03 gram). Subtracting the mass of beaker from the mass of beaker and beads, the mass of glass beads was found (i.e., ~16 gram). Since the beads are made of borosilicate glass (i.e., density of 2.23 g/cm³), the volume and mass of each bead were found to be approximately 0.00418 g/cm³ and 0.0093214 respectively. From these calculations, the number of beads in the beaker was calculated (i.e., ~1720).

An Abet LS-10500 solar simulator was used to apply a heat flux to the top surface of the beaker and mimic the effects of sun on water evaporation. The solar simulator is capable of creating a one sun output with a maximum beam size of 35 mm. A DC Xenon arc lamp produced the simulated solar light and fast F/1.0 fused silica condenser is used to collect radiation from lamp. The intensity of the flux can be manually adjusted and the intensity is inversely proportional to the beam diameter. In this experiment, a heat flux of approximately 1500 W/m² was applied and the beam size was maintained at 20 mm. A 90° beam tuner was used to apply the beam in a vertical position and impinge on the beaker. The heat flux produced by the solar simulator was measured with a 2.36-cm-diameter and 3.63-cm-high LI-200R pyranometer with a sensitivity of 75 µA per 1000 W/m². The pyranometer was mounted in a platform with labeling screw to adjust the orientation. The output of the pyranometer was measured with a LI-2500A light meter which was connected with the pyranometer with a 10 feet long BNC cable. The pyramnometer was used at the beginning and end of the experiment.

Since the capillary movement of water and subsequent drying is a critical mechanism, x-ray imaging was used to capture the image of water level and also evaluate the drying front during evaporation. The x-ray generator produced x-ray beams and a detector received the x-ray radiation. The x-ray generator (AP72) had a square opening of 8 cm by 8 cm and the detector (0822 xo/xp) had a rectangular dimension of 23 cm by 21 cm. The pixel size of the x-ray detector is 200- μ m and the energy capacity is 20kV-15 MV.

The schematic diagram of the experimental setup is presented in Figure 1. The distance between the x-ray generator and detector was maintained at 55 cm and the scale was placed

adjacent to the x-ray detector. The beaker with beads was placed on the scale with a negligible distance (~2 mm) from the x-ray detector in order to create a clearer image. The approximate distance between the beaker and x-ray generator was 52 cm. The distance between the solar simulator and the beaker was approximately 6 cm in vertical direction. A T-type thermocouple was inserted in the beads at a depth of 1 cm to measure the temperature of water during evaporation; a thermocouple holder was used to fix the thermocouple's position. The thermocouple was connected to an Agilent 34972A and the data were logged with Agilent Benchlink Data logger every 5 minutes.

At the beginning of the experiments, the beaker was placed on the scale, filled only with glass beads. An initial x-ray image was taken. Subsequently, the beaker was filled with 5.5 mL of water with the volumetric syringe dropper. From that point, the experiment was started and thermocouple was placed inside the beaker. Temperature and mass data were measured at 5 minute intervals. For the first 3 hours of the experiment, x-ray pictures were recorded every 20 minutes and then an additional picture at the beginning of the 4th hour. Subsequently, all x-ray images were captured every 8 hours. The x-ray generator was handled with a software called XIS to capture the picture by using a manual trigger with a frame time of 2000 ms. Three pictures at a single time frame were taken and the images were processed with Matlab. Using a Matlab code, all the pictures were subtracted from the initial, reference image (i.e., beaker and beads with no water). By subtracting from the reference image, the position of water level and also the drying front propagation during evaporation were found.

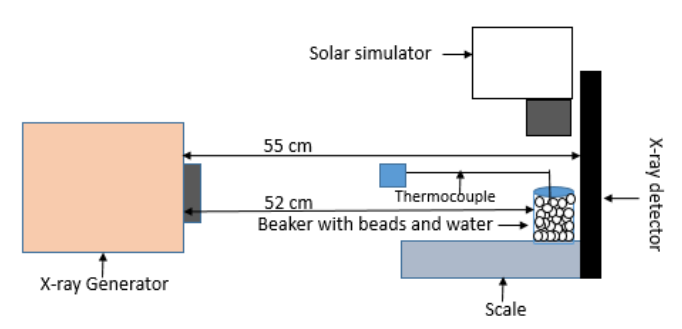


FIGURE 1: SCHEMATIC OF THE EXPERIMENTAL APPARATUS LOCATED IN AN ENVIRONMENTAL CHAMBER

3. RESULTS AND DISCUSSIONS

3.1 Evaporation Time

Evaporation experiments were conducted at fixed atmospheric conditions with $T=\sim22^{\circ}$ C, RH = $\sim35\%$ at a constant heat flux of 1500 W/m². The experiment was replicated three times to observe the repeatability of the evaporation phenomena. The evaporation times to evaporate 91% of the water (i.e., 5 mL out of a total of 5.5 mL) are shown in

Table 1. The experiments were lengthy; the average evaporation time to evaporate 5 mL of water was 2840 minutes (47.3 hours).

Table 1: Evaporation times to evaporate 5 mL of water (total 5.5 mL) for three replications

Replication	Evaporation time
	(minutes)
1	2850
2	2790
3	2880
Average	2840

3.2 Transient Mass Measurements

Initially, the water was slightly above the glass beads level and reduced due to transient evaporation. The mass loss of water during evaporation was recorded with a sensitive scale every 5 minutes during the experiment. Due to applied heat flux (\sim 1500 W/m²), the rate of evaporation was accelerated compared to field conditions. Evaporation data (i.e., decrease of mass, m, with respect to time, t) are presented in Figure 2 for evaporation of 5 mL of water; good repeatability is observed between the three replications. The slope (dm/dt) varies with respect to time, thereby indicating different evaporation stages.

To differentiate between three stages of evaporation, the average slopes (dm/dt) were calculated at each time t_0 using seven mass/time data points (i.e., averaged over a time interval of 30 minutes),

$$\left. \frac{\overline{dm}}{dt} \right|_{t_0} = \frac{\sum_{i=-3}^{i=3} (t_i - \overline{t})(m_i - \overline{m})}{(t_i - \overline{t})^2} \tag{1}$$

where m and t are mass of water and time, respectively, \overline{m} and \overline{t} are the averaged quantities over the half-hour interval, and i is the index. The evaporation process is generally slow; the maximum mass loss observed over a 30 minutes' period was 0.2 g. The average slopes are as shown in Figure 3.

From the mass data, the three stages of evaporation were observed during each replication. The steepest slope (i.e., largest evaporation rate) was observed at the beginning of the experiments; this corresponds to Stage I evaporation in which evaporation is dictated by evaporation at the surface [14, 15]. Evaporation rates in Stage 1 are around -0.005 g/min The average evaporation rate decreases between the 250 and 500 minute marks; this corresponds to a transition from Stage I to Stage II evaporation, in which evaporation rates are approximately -0.002 g/min. Evaporation rates decreases sharply as the evaporation process transitions from Stage II to Stage III evaporation [9, 16-22]. During Stage III evaporation, evaporation rates were as low as -0.0004 g/min (i.e., up to five times less than evaporation rates measured in Stage II evaporation). From this plot, the initial difference between three stages of evaporation can be observed and certain distinctions can be made with the basis of average mass loss. However, information about the evaporative front and partial dryout would yield more information about the mechanisms and will be investigated using x-rays.

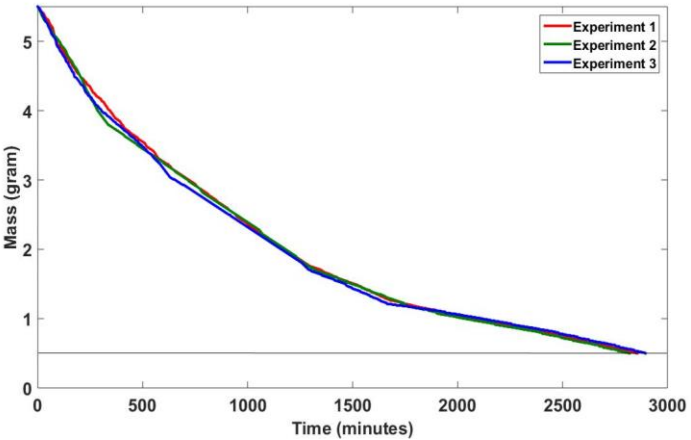


FIGURE 2: TRANSIENT MASS DECREASE DUE TO EVAPORATION

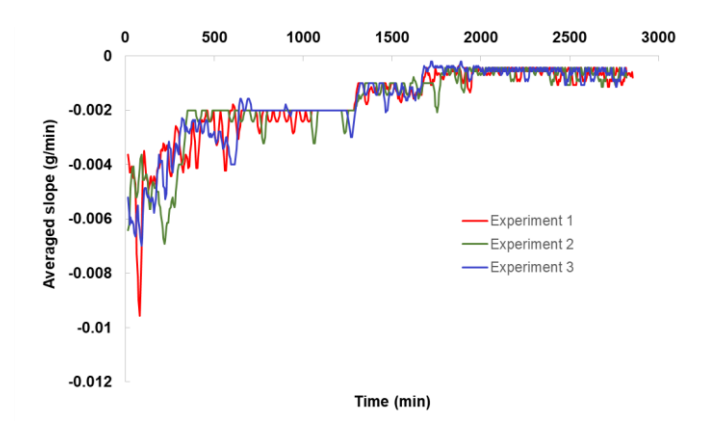


FIGURE 3: AVERAGE EVAPORATION RATES AS DETERMINED BY THE SLOPES OF THE MASS LOSS PER TIME GRAPH

3.3 Drying Front Imaging

X-ray imaging was used to observe the evaluation of drying front during evaporation. Initially, an image was taken using x-ray of the beaker with glass beads. Then, water was applied and the experiment was started; x-ray images were taken every 30 minutes for first 3 hours. An image was recorded at the 4th hour and subsequent pictures were captured every 8 hours. All the x-ray images were post processed with Matlab. The first step in processing the image was to normalize each image for the variation in fluxes from the x-ray generator. The value of each pixel in an image was then divided by the average value for a constant section of each image. The images were then analyzed by subtracting an image of the sample without water from the images with water so that only the water showed up on the image. A log transform of this image was performed to account for the exponential attenuation of the x-rays. This allowed for the area where there was water to be visible for each image.

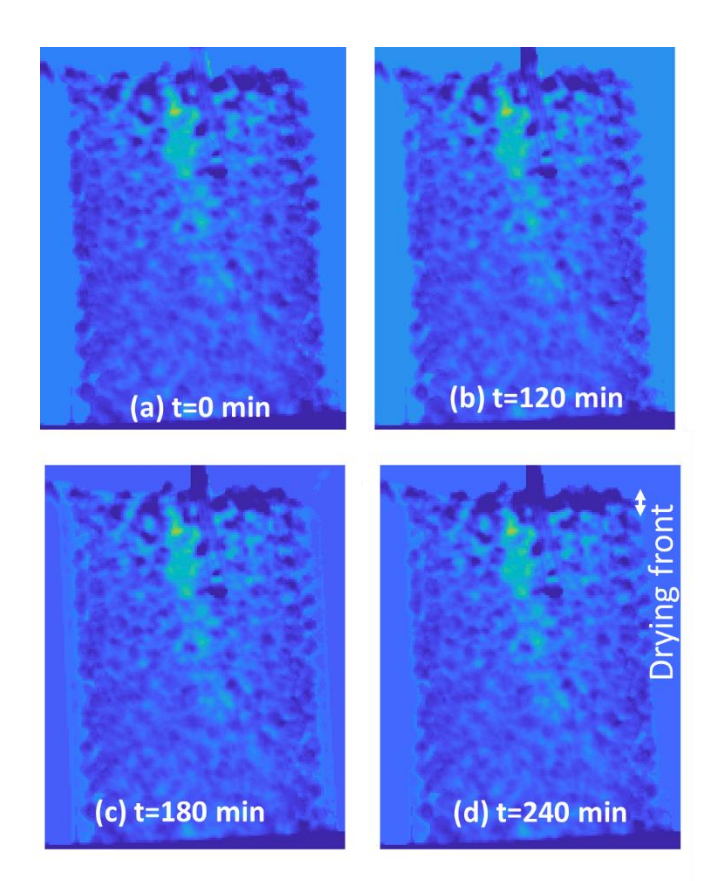


FIGURE 4: STAGE I EVAPORATION TRANSITIONING TO STAGE II EVAPORATION AT (A) TIMES OF *T*=0 MIN, (B) *T*=120 MIN, (C) *T*=180 MIN, AND (D) *T*=240 MIN.

Evaluation of the drying front is shown in the x-ray images presented in Figure 4. The beaker outline is visible. The light blue colors represent water and the deep blue areas represent the absence of water (i.e., the evaporative drying front). Initially, the water was slightly above the level of glass beads and the evaporation of that amount of water has slightest effect on x-ray imaging. Average evaporation rates, shown in Figure 3, were the highest during Stage I evaporation [Figure 4 (a), (b) (c)]. In these first three images, the dark blue color is constrained to the very top beads. Some water voids become more noticeable in Figure 4 (d) as the evaporation process transitions to Stage II evaporation. Transitioning from 240 minutes to 820 minutes, a noticeable difference of evaporative front can be seen indicative of Stage II evaporation (i.e., partial dryout). Approximately half of the water evaporates between 0 and 820 minutes and the change in drying front appeared to be significant [Figure 4(e)]. Approximately, 3 grams and 4.2 grams of water were evaporated after 1200 minutes and 1620 minutes, respectively and the significant increase in the drying front and transition between Stages II and III can be seen in Figure 4 (f) and (g). Transitioning from 1620 to 2810 minutes, the evaporation process slowed and consecutively the evaporation rate decreased, commensurate with the transition to Stage III evaporation. Figure 4 (h) shows the largest drying front length.

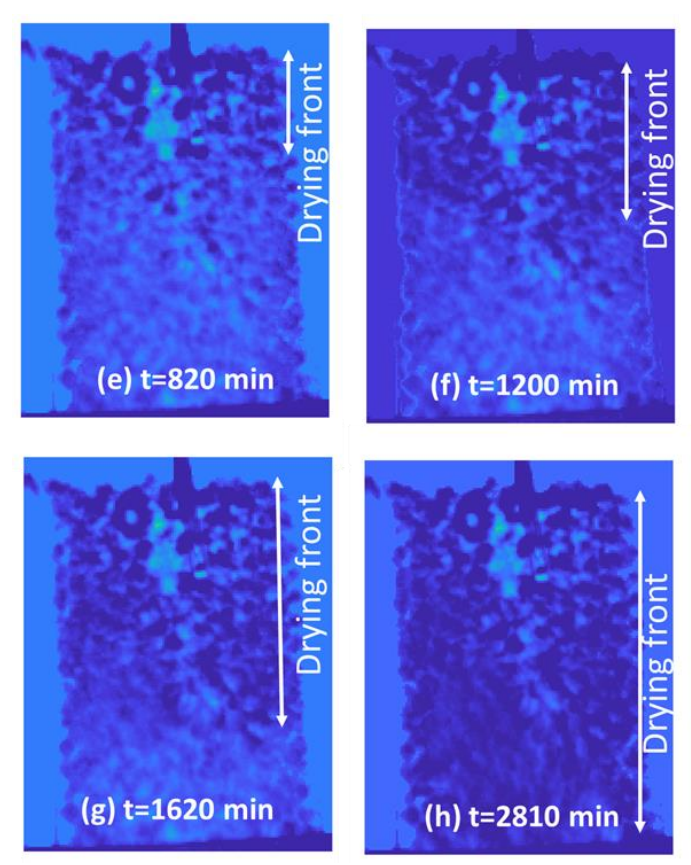


FIGURE 4: EVAPORATION/DRYING FRONT PROGRESSION DURING STAGE II EVAPORATION AND TRANSITION TO STAGE III EVAPORATION AT (E) TIMES OF T=820 MIN, (F) T=1200 MIN, (G) T=1620 MIN, AND (H) T=2810 MIN.

3.4 Evaporation stages

In order to further understand evaporation stages, average mass at 30 minute intervals were plotted against time (Figure 5). From the graph, it can be seen that, the Stage I evaporation is the fastest as the slope of this line is steep-most and takes least amount of time (~240 minutes). There is a transition period between stage I and II when the evaporation rate decreases. This transition happens between 240 to 600 minutes. There is a decrease in evaporation rate from Stage I to Stage II evaporation. Notably, approximately half of the water was evaporated before starting of this stage. Stage II persists through approximately ~1200 minutes. The significant difference in drying front in this stage can be observed from Figure 4 (f). In this stage, the mass loss reduces to ~0.01-0.02 grams. From around 1500 minutes, the evaporation process transitions to Stage III, which is the slowest among all three. The mass loss further reduces, and it takes approximately 20-25 minutes to evaporate 0.01 gram of water. Image (g) and (h) from Figure 4represent the drying front progression at 1620 and 2810 minutes, respectively. Due to the increase in the depth of drying front, evaporation by the bottom-level water is restricted to vapor diffusion. The last state of the evaporation can be seen from Figure 4 (h), where the depth of drying front is the largest and the amount of water was lowest. The experiments were terminated after 48 hours, although 0.5 mL remained.

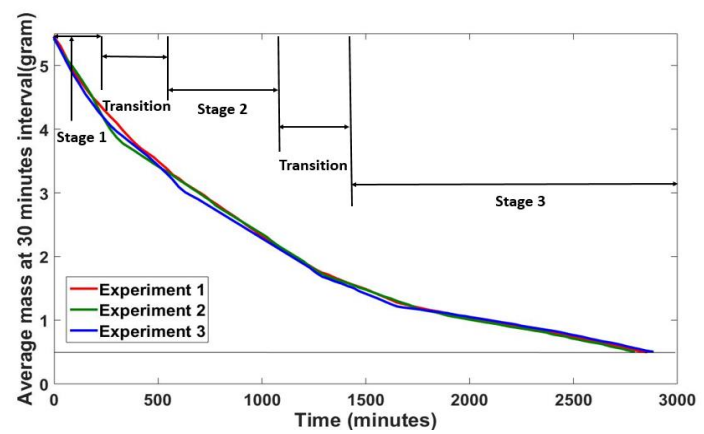


FIGURE 5: TRANSITIONS BETWEEN EVAPORATION STAGES I, II, AND III

3.5 Temperature data

A T-type thermocouple was used to record the temperature data, which were logged every five minutes. The thermocouple was inserted into the beads to a depth of 1 cm. Initially, the thermocouple was in contact with the beads and water. As the drying front increased more than 1 cm, only the tip temperature of the thermocouple was recorded and plotted against time (Figure 6). During the course of experiments, temperature varied from 23°C to 31° C. The average temperature was found ~28.5°C which was pretty consistent throughout the experiment. Therefore, the experiments can be approximated as isothermal.

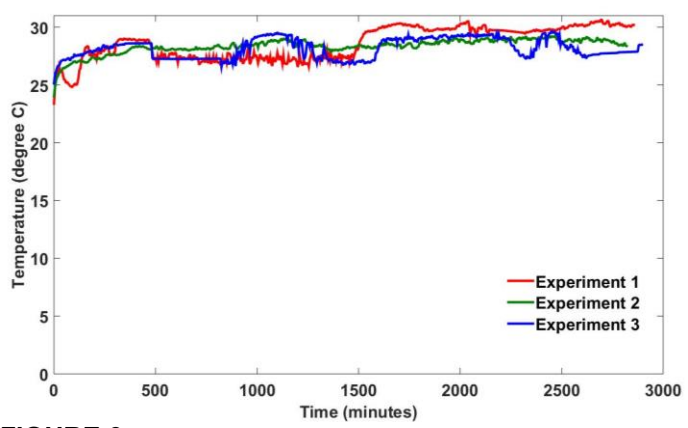


FIGURE 6: TEMPERATURE READINGS DURING THE 47-HOUR EXPERIMENTS

4. CONCLUSIONS

This paper investigated the evaporation of water from porous media (i.e., a beaker of hydrophilic glass beads used to simulate soil. Real time mass measurements were recorded, and x-ray imaging was used to observe the progression of the drying front in the beaker. Evaporation stages were determined from the combination of these measurements. Based on this research, the following conclusions can be drawn:

- All three evaporation stages were observed in this beaker.
- Evaporation rates in Stage 1 are around -0.005 g/min.
- The average evaporation rate decreases between the 250 and 500 minute marks; this corresponds to a transition

- from Stage I to Stage II evaporation, in which evaporation rates are approximately -0.002 g/min.
- Evaporation rates decreases sharply as the evaporation process transitions from Stage II to Stage III evaporation. During Stage III evaporation, evaporation rates were as low as -0.0004 g/min (i.e., up to five times less than evaporation rates measured in Stage II evaporation).
- Stage III evaporation corresponded to a drying front which encompassed nearly the entire beaker.

This research demonstrated that x-ray imaging is a viable tool to determine evaporation front propagation at this size scale. Future work will consider additional parameters (i.e., heat flux, bead size, etc.).

ACKNOWLEDGEMENTS

The authors gratefully acknowledge the support of NSF CAREER grant number 1651451.

REFERENCES

- [1] 2017, "World population projected to reach 9.8 billion in 2050, and 11.2 billion in 2100," https://www.un.org/development/desa/en/news/population/world-population-prospects-2017.html.
- [2] Oki, T., and Kanae, S., 2006, "Global hydrological cycles and world water resources," Science, 313(5790), pp. 1068-1072.
- [3] Wise, L., 2015, "A drying shame: With the Ogallala Aquifer in peril, the days of irrigation for western Kansas seem numbered,"

http://www.kansascity.com/news/state/kansas/article28640722.ht ml#storylink=cpy.

- [4] Steward, D. R., Bruss, P. J., Yang, X., Staggenborg, S. A., Welch, S. M., and Apley, M. D., 2013, "Tapping unsustainable groundwater stores for agricultural production in the High Plains Aquifer of Kansas, projections to 2110," Proceedings of the National Academy of Sciences, 110(37), pp. E3477-E3486.
- [5] Steward, D. R., and Allen, A. J., 2016, "Peak groundwater depletion in the High Plains Aquifer, projections from 1930 to 2110," Agricultural Water Management, 170, pp. 36-48
- [6] Gleeson, T., Alley, W. M., Allen, D. M., Sophocleous, M. A., Zhou, Y., Taniguchi, M., and VanderSteen, J., 2012, "Towards sustainable groundwater use: setting long-term goals, backcasting, and managing adaptively," Groundwater, 50(1), pp. 19-26.
- [7] Butler, J., Stotler, R., Whittemore, D., and Reboulet, E., 2013, "Interpretation of water level changes in the High Plains Aquifer in western Kansas," Groundwater, 51(2), pp. 180-190.
- [8] Jury, W. A., and Horton, R., 2004, Soil physics, John Wiley & Sons.
- [9] Hillel, D., 1998, Environmental soil physics, Academic Press, San Diego, CA.
- [10] Bittelli, M., Ventura, F., Campbell, G. S., Snyder, R. L., Gallegati, F., and Pisa, P. R., 2008, "Coupling of heat, water vapor, and liquid water fluxes to compute evaporation in bare soils," Journal of Hydrology, 362(3), pp. 191-205.
- [11] Cary, J., 1964, "An evaporation experiment and its irreversible thermodynamics," International Journal of Heat and Mass Transfer, 7(5), pp. 531-538.

- [12] Sakai, M., Toride, N., and Šimůnek, J., 2009, "Water and vapor movement with condensation and evaporation in a sandy column," Soil Science Society of America Journal, 73(3), pp. 707-717.
- [13] Sartori, E., 2000, "A critical review on equations employed for the calculation of the evaporation rate from free water surfaces," Solar Energy, 68(1), pp. 77-89.
- [14] Jones, F. E., 1991, Evaporation of water with emphasis on applications and measurements, CRC Press.
- [15] Penman, H. L., "Natural evaporation from open water, bare soil and grass," Proc. of the Royal Society of London A: Mathematical, Physical and Engineering Sciences, The Royal Society, pp. 120-145.
- [16] Or, D., Lehmann, P., Shahraeeni, E., and Shokri, N., 2013, "Advances in soil evaporation physics—A review," Vadose Zone Journal, 12(4), pp. 1-16.
- [17] Shokri, N., Lehmann, P., and Or, D., 2009, "Characteristics of evaporation from partially wettable porous media," Water Resources Research, 45(2), p. W02415.
- [18] Shokri, N., Lehmann, P., and Or, D., 2009, "Critical evaluation of enhancement factors for vapor transport through unsaturated porous media," Water Resources Research, 45(10), p. W10433.
- [19] Shokri, N., Lehmann, P., and Or, D., 2008, "Effects of hydrophobic layers on evaporation from porous media," Geophysical Research Letters, 35(19), p. L19407.

- [20] Salvucci, G. D., 1997, "Soil and moisture independent estimation of stage-two evaporation from potential evaporation and albedo or surface temperature," Water Resources Research, 33(1), pp. 111-122.
- [21] Suleiman, A., and Ritchie, J., 2003, "Modeling soil water redistribution during second-stage evaporation," Soil Science Society of America Journal, 67(2), pp. 377-386.
- [22] Shokri, N., and Or, D., 2011, "What determines drying rates at the onset of diffusion controlled stage-2 evaporation from porous media?," Water Resources Research, 47(9), p. W09513.
- [23] Jury, W., and Letey, J., 1979, "Water vapor movement in soil: reconciliation of theory and experiment," Soil Science Society of America Journal, 43(5), pp. 823-827.
- [24] Cary, J., 1963, "Onsage's relation and the non-isothermal diffusion of water vapor," The Journal of Physical Chemistry, 67(1), pp. 126-129.
- [25] Lu, S., Ren, T., Yu, Z., and Horton, R., 2011, "A method to estimate the water vapour enhancement factor in soil," European Journal of Soil Science, 62(4), pp. 498-504.
- [26] Philip, J., and De Vries, D., 1957, "Moisture movement in porous materials under temperature gradients," Eos, Transactions American Geophysical Union, 38(2), pp. 222-232.
- [27] De Vries, D., 1958, "Simultaneous transfer of heat and moisture in porous media," Eos, Transactions American Geophysical Union, 39(5), pp. 909-916.